УНИВЕРСИТЕТ ИТМО
НАУЧНО-ТЕХНИЧЕСКИЙ ВЕСТНИК ИНФОРМАЦИОННЫХ ТЕХНОЛОГИЙ, МЕХАНИКИ И ОПТИКИ
январь–февраль 2022 Том 22 № 1 http://ntv.ifmo.ru/
SCIENTIFIC AND TECHNICAL JOURNAL OF INFORMATION TECHNOLOGIES, MECHANICS AND OPTICS
January–February 2022 Vol. 22 No 1 http://ntv.ifmo.ru/en/
ISSN 2226-1494 (print) ISSN 2500-0373 (online)
НАУЧНО-ТЕХНИЧЕСКИЙ ВЕСТНИК ИНФОРМАЦИОННЫХ ТЕХНОЛОГИЙ, МЕХАНИКИ И ОПТИКИ

doi: 10.17586/2226-1494-2022-22-1-147-154

A new analytical model of drain current and small signal parameters for AlGaN-GaN high-electron-mobility transistors

Azzeddine Farti[1]✉, Abdelkader Touhami[2]

[1,2] Hassan II University of Casablanca, Casablanca, 20190, Morocco

[1] azzeddine.farti-etu@etu.univh2c.ma✉, https://orcid.org/0000-0002-8694-1471
[2] abdelkadertouhami2016@gmail.com, https://orcid.org/0000-0001-8582-1884

Abstract
The paper proposes a new analytical model of the drain current in AlGaN-GaN high-electron-mobility transistors (HEMT) on the basis of a polynomial expression for the Fermi level as a function of the concentration of charge carriers. The study investigated the influence of parasitic resistances (source and drain sides), high-speed saturation, the amount of aluminum in the AlGaN barrier, and low field mobility. To isolate the output characteristics, cut-off frequency and steepness, the parameters of the hyper frequency signal were developed. Comparison of analytical calculations with experimental measurements confirmed the validity of the proposed model.

Keywords
AlGaN-GaN, HEMTs, 2-DEG two-dimensional electron gas, current–voltage characteristics, cut-off frequencies, Transconductance

Acknowledgements
This work carried out at the Faculty of Sciences Ain Chok Km 8, Hassan II University, Casablanca, Morocco.

For citation: Farti A., Touhami A. A new analytical model of drain current and small signal parameters for AlGaN-GaN high-electron-mobility transistors. *Scientific and Technical Journal of Information Technologies, Mechanics and Optics*, 2022, vol. 22, no. 1, pp. 147–154. doi: 10.17586/2226-1494-2022-22-1-147-154

УДК 621.382.3

Новая аналитическая модель тока стока и параметров малых сигналов AlGaN-GaN транзисторов с высокой подвижностью электронов

Азеддин Фарти[1]✉, Абделькадер Тухами[2]

[1,2] Университет Хасана II, Факультет наук Касабланки, Касабланка, 20190, Марокко

[1] azzeddine.farti-etu@etu.univh2c.ma✉, https://orcid.org/0000-0002-8694-1471
[2] abdelkadertouhami2016@gmail.com, https://orcid.org/0000-0001-8582-1884

Аннотация
Предложена новая аналитическая модель тока стока в устройствах AlGaN-GaN транзисторов с высокой подвижностью электронов (HEMT) на основе полиномиального выражения для уровня Ферми как функции концентрации носителей заряда. В ходе исследования изучено влияние паразитных сопротивлений (стороны истока и стока), высокоскоростного насыщения, количества алюминия в барьере AlGaN и низкой подвижности поля. Для выделения выходных характеристик, частоты среза и крутизны разработаны параметры гиперчастотного сигнала. Сравнение аналитических расчетов с экспериментальными измерениями подтвердило справедливость предложенной модели.

Ключевые слова
AlGaN-GaN, транзистор с высокой подвижностью электронов, HEMT, двумерный электронный газ, вольтамперная характеристика, частота среза, крутизна характеристики

Благодарности
Работа выполнена на факультете наук Айн Чок Km 8, Университет Хасана II, Касабланка, Марокко.

© Farti A., Touhami A., 2022

Ссылка для цитирования: Фарти А., Тухами А. Новая аналитическая модель тока стока и параметров малых сигналов AlGaN-GaN транзисторов с высокой подвижностью электронов // Научно-технический вестник информационных технологий, механики и оптики. 2022. Т. 22, № 1. С. 147–154 (на англ. яз.). doi: 10.17586/2226-1494-2022-22-1-147-154

Introduction

High-electron-mobility transistors (HEMT) based on the AlGaN-GaN hetero-structure have rapidly emerged in the fabrication of very high-speed integrated circuits [1]. These transistors have taken an important place in the realization of high-power, high-voltage, and high-temperature devices because of their very tall switching speed, poor power consumption and relatively easy manufacturing technology.

Due to their considerable gap energy and significant discontinuity of conduction bands between the AlGaN and GaN layers, HEMT transistors can create a two-dimensional electron gas (2-DEG), with a concentration in the order of 10^{13} cm^{-2} under the spontaneous polarization effect and the piezoelectric effect [2].

To develop a reliable model for HEMT transistors, an accurate estimate of the 2-DEG density at the hetero-interface is significant. A number of charge control models for HEMTs and several theoretical models of drain current in HEMT transistors have been developed to characterize the concentration of the two-dimensional electron's gas (2-DEG) at the AlGaN-GaN interface [2–6].

The previous work on theoretical analysis of HEMT AlGaN-GaN [5] has been done by solving simultaneously the Schrödinger and Poisson equations. According to the assumption's authors, the polarization in nitride alloys interpolates linearly [7]; meanwhile, Fiorentini et al [8] have argued that there is a significant variety in the theoretical results when nonlinear polarization is applied instead of linear polarization. This can be explained by the fact that nonlinearity modifies the interface charge densities induced by the polarization. Analyzing the models involving polarization nonlinearity [9–12], we found that theoretical models are not suitable with the experimental result (the current-voltage characteristic and the transconductance).

In the paper, we present a new model of charge control using the 2-DEG channel current equation developed by Rashmi et al [5], and considering the nonlinearity of the polarization which will produce a good optimization with the experimental result. In this model we also introduce the Fermi level $E_F(T, m)$ in its simple polynomial form as a function of the electron gas density $n_s(T, m)$.

Based on the proposed analytical model, we will extract the current-voltage characteristics and describe the variations of the channel transconductance of the device. To highlight the performance and operating limits of HEMT transistors at microwave frequencies, first, we study the variation of cut-off frequencies f_T and the transcanductance g_m as a function of the drain current at fixed drain voltage, and secondly, we analyze the variation of the cut-off frequency as a function of the bias voltages V_{ds} and V_{gs}.

Model formulation

Charge-control model

The structure of HEMT mainly consists of three different materials: substrate, material with a wide bandgap, and material with a low bandgap. The junction of these two materials leads to the formation of two-dimensional electron gas (2-DEG) at the interface. It can be modulated by the gate-source voltage, while the formation of the electron gas is performed between the spacer and the small gap layer (Fig. 1). The sheet carrier concentration of the two-dimensional electron gas (2-DEG) constituted at the AlGaN-GaN heterojunction is given by [9]:

$$n_s(T, m) = \frac{\varepsilon(m)}{qd}(V_{gs} - V_{th}(T, m) - E_F(T, m)), \quad (1)$$

where T is the temperature; m is the Al mole fraction in AlGaN-GaN; q is the electron charge; $\varepsilon(m)$ is the dielectric constant of $Al_mGa_{1-m}N$; d is the summation of the doped AlGaN layer thickness (d_d) and the undoped AlGaN spacer layer thickness (d_i). $V_{th}(m)$ is the threshold voltage, $E_F(T, m)$ is the position of the Fermi level which is expressed as a function of $n_s(T, m)$ and it is given by the form of a simple polynomial [13].

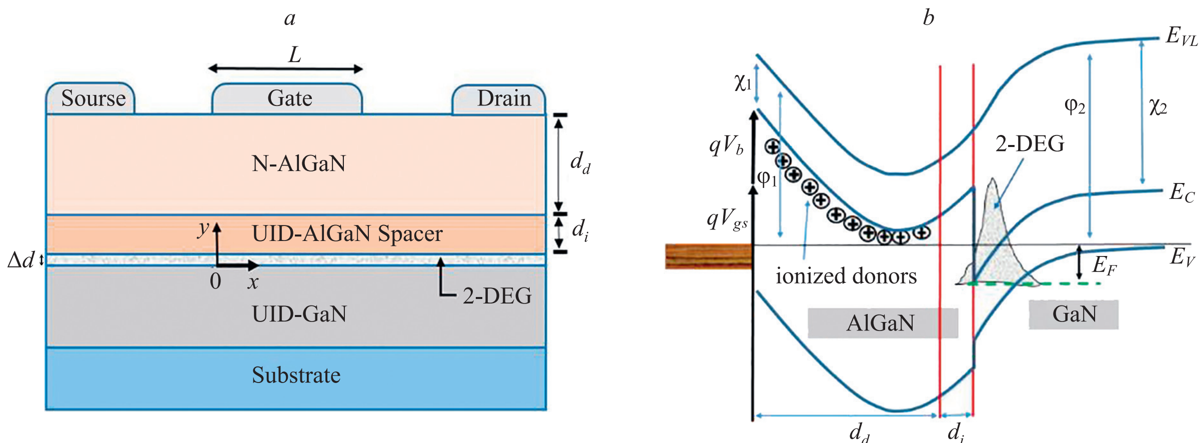

Fig. 1. HEMT transistor AlGaN-GaN in cross-section (*a*) and the band diagram of the AlGaN-GaN structure (*b*)

$$E_F(T, m) = K_1(T) + K_2(T)\sqrt{n_s(T, m)} + K_3(T)n_s(T, m), \quad (2)$$

where K_1, K_2 and K_3 are three different parameters depending on the temperature T.

Where L is the Gate length, x present the position along the transistor channel. V_b presents the Schottky-barrier height, φ_1 and φ_2 are work functions of AlGaN and GaN, respectively. χ_1 (χ_2) is electron affinity of AlGaN (GaN). E_{VL}, E_C and E_V show the vacuum level, the energy of the conduction band, the energy of the valence band, respectively.

By introducing the equation (2) into (1), we obtained a quadratic equation, to demonstrate the concentration of 2-DEG charge carriers at the heterojunction [14].

$$n_s(T, m) = \left(\frac{-K_2(T) + \sqrt{K_2^2(T) + 4K_4(T, m)(V_{gs} - V_{th}(T, m) - K_1(T))}}{2K_4(T, m)}\right)^2, \quad (3)$$

where

$$K_4(T, m) = K_3(T) + \frac{qd}{\varepsilon(m)}.$$

The threshold voltage $V_{th}(T, m)$ depends on the aluminum mole fraction of MOSFET, and its expression given by [15].

$$V_{th}(T, m) = \varphi(m) - \Delta E_C(T, m) - \frac{qN_d d_d^2}{2\varepsilon(m)} - \frac{\sigma_{PZ}(m)}{\varepsilon(m)}d,$$

where $\varphi(m)$, $\Delta E_C(m)$ are the Schottky barrier height and conduction band discontinuity between GaN and AlGaN, respectively. N_d is the doping density of the Al-Ga-N layer and $\sigma_{PZ}(m)$ is the charge density induced by the total polarization, can be written as follows [8]:

$$\sigma_{PZ}(m) = |P_{PP}(m) + P^{sp}_{\mathrm{Al}_m\mathrm{Ga}_{1-m}\mathrm{N}}(m) - P^{sp}_{\mathrm{Al}_m\mathrm{Ga}_{1-m}\mathrm{N}}(0)|,$$

where $P_{PP}(m)$ is the piezo-electric polarization with its expression and it varies as a function of the value of m. $P^{sp}_{\mathrm{Al}_m\mathrm{Ga}_{1-m}\mathrm{N}}(m)$ and $P^{sp}_{\mathrm{Al}_m\mathrm{Ga}_{1-m}\mathrm{N}}(0)$ are the spontaneous polarizations of $\mathrm{Al}_m\mathrm{Ga}_{1-m}\mathrm{N}$ and GaN, respectively [8].

$$P_{PP}(m) = \begin{cases} P^{pz}_{\mathrm{Al}_m\mathrm{Ga}_{1-m}\mathrm{N}}(m) & \text{For } 0 \le m < 0.38 \\ P^{pz}_{\mathrm{Al}_m\mathrm{Ga}_{1-m}\mathrm{N}}(2.33\text{–}3.5m) & \text{For } 0.38 \le m \le 0.67, \\ 0 & \text{For } 0.67 \le m \le 1 \end{cases}$$

The expressions of spontaneous and piezo-electric polarizations are given in Table 1 [8].

Current–voltage characteristics ($I_{ds} - V_{ds}$)

By fixing the value of voltage V_{ds} superior of the threshold voltage, the electron movement at the AlGaN/GaN interface is ensured by the application of the source-drain voltage V_{ds} superior to zero. The generated drain current I_{ds} is given by the following equation [5].

$$I_{ds}(T, m, x) = Zq\mu(x)\left(n_s(T, m)\frac{dV_C(x)}{dx} + \frac{K_B T}{q}\frac{dn_s(T, m)}{dx}\right), \quad (4)$$

where Z, $V_C(x)$ and K_B are the gate width, the channel potential at position x, and Boltzmann's constant, respectively. $\mu(x)$ is the field dependent of the mobility given by:

$$\mu(x) = \frac{\mu_0}{\left(1 + \frac{(\mu_0 E_C - v_{sat})}{E_C v_{sat}}\frac{dV_C(x)}{dx}\right)}, \quad (5)$$

where E_C is the saturation electric field, μ_0 is the low-field mobility, and v_{sat} is the saturation drift velocity.

Depending on the variation of the bias voltage V_{ds}, the HEMT transistor can be function under two different regimes (linear regime and saturation regime).

The linear region ($V_{ds} < V_{dsat}$)

To describe the variation of potential at each position x in the 2-DEG channel, the voltage V_{gs} is replaced by $V_{gs} - V_C(x)$ in the expression (3) of sheet carrier concentration of two-dimensional electron gas formed at the AlGaN/GaN heterojunction.

$$n_s(T, m, x) = \left(\frac{-K_2(T)}{2K_4(T, m)} + \frac{\sqrt{K_2^2(T) + 4K_4(T, m)(V_{gs} - V_{th}(T, m) - V_C(x) - K_1(T))}}{2K_4(T, m)}\right)^2. \quad (6)$$

Using the following approximation [16] in equation (6) we get:

$$4K_4(T, m)V_C(x) << K_2^2(T) + 4K_4(T, m)(V_{gs} - V_{th}(T, m) - K_1(T)).$$

After using the above given approximation in equation (6), a simple expression of the concentration $n_s(T, m)$ have the following form:

$$n_s(T, m) = \left(\frac{-K_2(T) + \sqrt{K_2^2(T) + 4K_4(T, m)(V_{gs} - V_{th}(T, m) - K_1(T))}}{2K_4(T, m)}\right)^2. \quad (7)$$

Table 1. Parameters of the $\mathrm{Al}_m\mathrm{Ga}_{1-m}\mathrm{N}$/GaN heterostructure

Description	Parameter	Expression
Spontaneous polarization of AlGaN	$P^{sp}_{\mathrm{Al}_m\mathrm{Ga}_{1-m}\mathrm{N}}(m)$, C/m^2	$-0.09m - 0.034(1 - m) + 0.019m(1 - m)$
Piezo-electric polarization of AlGaN	$P^{pz}_{\mathrm{Al}_m\mathrm{Ga}_{1-m}\mathrm{N}}(m)$, C/m^2	$mP^{pz}_{\mathrm{AlN}}[\varepsilon_b(m)] + (1 - m)P^{pz}_{\mathrm{GaN}}[\varepsilon_b(m)]$
Piezo-electric polarization of AlN	$P^{pz}_{\mathrm{AlN}}(m)$, C/m^2	$-1.808\varepsilon_b(m) + 5.624\varepsilon_b^2(m)$
Piezo-electric polarization of GaN	$P^{pz}_{\mathrm{GaN}}(m)$, C/m^2	$-0.918\varepsilon_b(m) + 9.541\varepsilon_b^2(m)$
The basal strain	$\varepsilon_b(m)$	$(a(0) - a(m))/a(m)$
The lattice constant	$a(m)$, nm	$0.031986 - 0.000891m$

Consequently, the drain current from equation (4) will be expressed by:

$$I_{ds}(T, m, x) = Zq\mu(x)\left(n_s(T, m)\frac{dV_C(x)}{dx}\right). \quad (8)$$

We substitute the equations (5) and (7) in the drain current equation (8), and a new equation will appear which describes the drain current at each position x of the channel:

$$I_{ds}(T, m, x) = Zq\mu_0 \times$$
$$\times \left(\frac{-K_2(T) + \sqrt{K_2^2(T) + 4K_4(m)(V_{gs} - V_{th}(m) - K_1(T)}}{2K_4(T, m)}\right)^2 \times$$
$$\times \frac{\frac{dV_C(x)}{dx}}{\left(1 + \frac{(\mu_0 E_C - v_{sat})}{E_C v_{sat}}\frac{dV_C(x)}{dx}\right)}. \quad (9)$$

Fig. 2 shows the equivalent electrical circuit diagram of the high-electron-mobility transistor HEMT (AlGaN-GaN), where R_s and R_d are the parasitic resistances of the source and drain, respectively. R_c represents the resistance of the 2-DEG channel.

From the schema in Fig. 2, the channel potential for $x = 0$ and $x = L$ will be given by:

$$V_C(x)|_{x=0} = I_{ds}R_s,$$
$$V_C(x)|_{x=L} = V_{ds} - (I_{ds}R_d).$$

With the above given boundary conditions, the various steps of integration of the equation (9) along the transistor channel will be written as follows:

$$I_{ds}\int_0^L \left(1 + \frac{(\mu_0 E_C - v_{sat})}{E_C v_{sat}}\frac{dV_C(x)}{dx}\right)dx =$$
$$= Zqn_s(T, m)\mu_0\int_0^L \left(\frac{dV_C(x)}{dx}\right)dx,$$
$$I_{ds}\left([x]_0^L + \frac{(\mu_0 E_C - v_{sat})}{E_C v_{sat}}[V_C(x)]_0^L\right) = Zqn_s(T, m)\mu_0[V_C(x)]_0^L,$$
$$-I_{ds}^2\left(\frac{(\mu_0 E_C - v_{sat})}{E_C v_{sat}}(R_s + R_d)\right) +$$
$$+ I_{ds}\left(L + \frac{(\mu_0 E_C - v_{sat})}{E_C v_{sat}}V_{ds} + Zqn_s(T, m)\mu_0(R_s + R_d)\right) - \quad (10)$$
$$- Zqn_s(T, m)\mu_0 V_{ds} = 0.$$

From equation (10), by replacing $ns(T, m)$ with its value, the first term is multiplied by I_{ds}^2 into α_1, the second term is multiplied by I_{ds} into α_2 and the last term that does not contain I_{ds} by α_3, we can obtain:

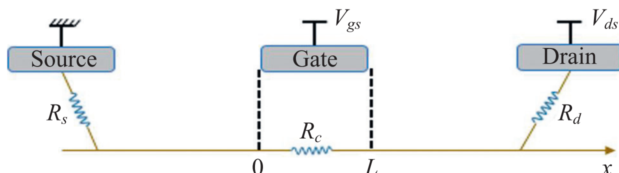

Fig. 2. Equivalent electrical schema of the HEMT

$$\alpha_1 = -\left(\frac{(\mu_0 E_C - v_{sat})}{E_C v_{sat}}(R_s + R_d)\right),$$
$$\alpha_2 = L + Zq\mu_0(R_s + R_d)\times$$
$$\times \left(\frac{-K_2(T) + \sqrt{K_2^2(T) + 4K_4(T)(V_{gs} - V_{th}(T, m) - K_1(T))}}{2K_4(T)}\right)^2 +$$
$$+ \frac{(\mu_0 E_C - v_{sat})}{E_C v_{sat}}V_{ds}, \quad (11)$$
$$\alpha_3 = -Zq\mu_0 \times \quad (12)$$
$$\times\left(\frac{-K_2(T) + \sqrt{K_2^2(T) + 4K_4(T, m)(V_{gs} - V_{th}(T, m) - K_1(T))}}{2K_4(T, m)}\right)^2 \times$$
$$\times V_{ds}.$$

The expression of the drain current I_{ds} in linear regime will be given by the root of equation (10) and can be written in the following form:

$$I_{ds} = \frac{-\alpha_2 + \sqrt{\alpha_2^2 - 4\alpha_1\alpha_3}}{2\alpha_1}.$$

The saturation region ($V_{ds} \geq V_{dsat}$)

The application of an electric field in a semiconductor leads to free charge carriers (electrons and holes) to acquire a velocity of displacement υ proportional to the applied field. The following relationship describes this velocity:

$$\upsilon = \mu(x)E(x) = \frac{\mu_0}{\left(1 + \frac{(\mu_0 E_C - v_{sat})}{E_C v_{sat}}\frac{dV_C(x)}{dx}\right)}\frac{dV_C(x)}{dx}.$$

At high electric field values, the velocity of the carriers is saturated at the value υ_{sat}. This fact has allowed us to replace the velocity υ by υ_{sat} in expression (9) of the drain current I_{ds}:

$$I_{dsat} = Zq\upsilon_{sat} \times \quad (13)$$
$$\times \left(\frac{-K_2(T) + \sqrt{K_2^2(T) + 4K_4(T, m)(V_{gs} - V_{th}(T, m) - K_1(T))}}{2K_4(T, m)}\right)^2.$$

In the same way, we replace the voltage V_{ds} by the saturation voltage V_{dsat} in the equations (11) and (12).

In this case, the expression of the drain current in the saturation regime can be written in the form:

$$I_{dsat} = \frac{-\beta_2 + \sqrt{\beta_2^2 - 4\alpha_1\beta_3}}{2\alpha_1}, \quad (14)$$

With,

$$\beta_2 = \delta_2 + \frac{(\mu_0 E_C - v_{sat})}{E_C v_{sat}}V_{dsat}, \quad (15)$$

and

$$\beta_3 = \delta_3 V_{dsat}, \quad (16)$$

where

$$\delta_2 = L + Zq\mu_0(R_s + R_d) \times$$
$$\times\left(\frac{-K_2(T) + \sqrt{K_2^2(T) + 4K_4(T, m)(V_{gs} - V_{th}(T, m) - K_1(T))}}{2K_4(T, m)}\right)^2,$$
$$\delta_3 = -Zq\mu_0 \times$$
$$\times\left(\frac{-K_2(T) + \sqrt{K_2^2(T) + 4K_4(T, m)(V_{gs} - V_{th}(T, m) - K_1(T))}}{2K_4(T, m)}\right)^2.$$

To determine the expression of the saturation voltage V_{dsat}, we equalize the equations (13) and (14) of the drain current I_{ds}:

$$\frac{-\beta_2 + \sqrt{\beta_2^2 - 4\alpha_1\beta_3}}{2\alpha_1} = Zq\upsilon_{sat} \times \quad (17)$$
$$\times\left(\frac{-K_2(T) + \sqrt{K_2^2(T) + 4K_4(T, m)(V_{gs} - V_{th}(T, m) - K_1(T))}}{2K_4(T, m)}\right)^2.$$

We put:

$$\delta_1 = 2\alpha_1 Zqv_{sat} \times$$
$$\times\left(\frac{-K_2(T) + \sqrt{K_2^2(T) + 4K_4(T, m)(V_{gs} - V_{th}(T, m) - K_1(T))}}{2K_4(T, m)}\right)^2,$$

And equation (17) will be described as:

$$-\beta_2 + \sqrt{\beta_2^2 - 4\alpha_1\beta_3} = \delta_1. \quad (18)$$

According to the expressions of (15) and (16), equation (18) is as follows:

$$\delta_1 = -\left(\delta_2 + \frac{(\mu_0 E_C - v_{sat})}{E_C v_{sat}}V_{dsat}\right) +$$
$$+\sqrt{\left(\delta_2 + \frac{(\mu_0 E_C - v_{sat})}{E_C v_{sat}}V_{dsat}\right)^2 - 4\alpha_1\delta_3 V_{dsat}},$$

As a result, the expression of the saturation voltage V_{dsat} can be deduced and expressed by the formula:

$$V_{dsat} = \frac{-\delta_1(2\delta_2 + \delta_1)}{\left(2\delta_1\dfrac{(\mu_0 E_C - v_{sat})}{E_C v_{sat}} + 4\alpha_1\delta_3\right)}.$$

Small signal parameters

At this stage, for better modelling of the HEMT transistor, we need to determine and calculate its small signals parameters like the transconductance g_m and the cut-off frequency f_T, which may reflect the performance of this transistor.

Transconductance g_m

The transconductance is considered as one of the most important parameters in evaluating the performance of transistors for high-frequency applications. The transconductance g_m of the $Al_mGa_{1-m}N/GaN$ HEMT transistor is defined as [17].

$$g_m = \left.\frac{\partial I_{ds}}{\partial V_{gs}}\right|_{V_{ds}=cte}, \quad (19)$$

where:

$$I_{ds} = \frac{-\alpha_2 + \sqrt{\alpha_2^2 - 4\alpha_1\alpha_3}}{2\alpha_1}, \quad (20)$$

From (19) and (20), we obtained the expression of the transconductance written by the equation:

$$g_m = \frac{1}{2\alpha_1}\left(-\frac{\partial\alpha_2}{\partial V_{gs}} + \frac{2\alpha_2\dfrac{\partial\alpha_2}{\partial V_{gs}} - 4\alpha_1\dfrac{\partial\alpha_3}{\partial V_{gs}}}{2\sqrt{\alpha_2^2 - 4\alpha_1\alpha_3}}\right).$$

Cut-off frequency f_T

The characterization of the high-frequency performance of the HEMT transistor requires a detailed study of its cut-off frequency f_T. This later determines the factor of the microwave operation of HEMT transistor components. The cut-off frequency can be calculated versus the transconductance g_m as follows [10]:

$$f_T = \frac{g_m\mu_0}{2\pi L\dfrac{Z\mu_0\varepsilon(m)}{(d_d + d_i + \Delta d)}}, \quad (21)$$

where Δd presents the thickness of two-dimensional electron gas 2-DEG.

Results and discussion

To highlight the models of electrical and technological parameters (I_{ds}, g_m and f_T) of the HEMT transistor, we made a comparison with experimental results [18]. The electrical, geometrical and technological parameters used in the proposed model are presented in Table 2.

The values of the constants K_1, K_2 and K_3 used in the theoretical calculations for different values of the gate voltage V_{gs} with $m = 0.15$ are depicted in Table 3.

Fig. 3 shows the electrical characteristics of the HEMT transistor ($Al_{0.15}Ga_{0.85}N/GaN$) as compared to experimental measurements [18]. The length and the width gate of this transistor are equal to 1 μm and 75 μm, respectively. Fig. 3, *a* shows the variation of the drain current as a function of the drain voltage for different values of the gate voltage. For the calculation, we took a gate voltage sweep between –2 V and 1 V with a step of 1 V.

The results of the simulation indicate that there are two operating regimes. The first one is a linear regime, implying that the drain voltage increases, then the drain current I_{ds}

Table 2. Different parameters used in the proposed model

Parameter	Description	Value
V_{th}, V	Threshold voltage	–2.6
d_d, nm	Thickness of the doped layer	22
d_i, nm	Thickness of the undoped layer	3
Z, μm	Gate width	75
L, μm	Gate length	1
V_{sat}, m/s	Saturation velocity	1.19×10^5
R_s, Ω	Parasitic source resistance	0.6
R_d, Ω	Parasitic drain resistance	0.9

Table 3. Values of the parameters K_1, K_2 and K_3 for different gate voltage values V_{gs}. They are calculated with the same method [19] using the effective mass $m^* = 0.22m_0$ [7]

Gate voltage , V_{gs}, V	K_1, V	$K_2 \times 10^{-8}$, V·m	$K_3 \times 10^{-18}$, V·m^2
1	–0.27750	1.68742	–4.23715
0	–0.27573	1.45776	–3.21042
–1	–0.27423	1.26515	–2.34936
–2	–0.27422	1.26274	–2.33856

also increases. In a saturated regime, the drain current keeps constant and independent to the drain voltage V_{ds}. This can be explained by the pinching of the canal and the saturation of the electron velocity. These results coincide with the experimental measurements and prove the validity of the proposed model.

The curve in Fig. 3, *b* represents the dependence of the drain current vs. the gate voltage for a drain voltage set at the value 5V. We concluded that the intersection of the asymptote of the curve with the axis of the voltages V_{gs} is equal to –2.6 V. This value is equivalent to the threshold voltage V_{th} of the HEMT transistor under study. In other words, the results of our model are in concordance with the experimental data and confirm the validity of our model.

Fig. 3, c displays the variation of the transconductance g_m as a function of the gate voltage V_{gs} with the value of the drain voltage V_{ds} equal to 5 V. This transconductance g_m increases with the voltage V_{gs} till it reaches a maximum g_{mMax} (160 mS/mm) for the value of the gate voltage equal to –0.74 V. Consequently, the HEMT transistor achieves its optimum operating point. After this maximum, the transconductance decreases progressively, which can be attributed to the saturation of the carrier's velocity and the reduction of their mobility in the channel. This is caused by the increase in channel resistance. In addition, the thermal effects and presence of defects can be responsible for this drop transconductance.

Fig. 4, *a* shows the cut-off frequencies f_T and the transcanductance g_m as a function of the drain current I_{ds} with gate width $Z = 2 \times 75$ µm and the fixed drain voltage V_{ds} = 5V. We observe that the maximum of the cut-off frequency is 9.66 GHz which corresponds to a drain current

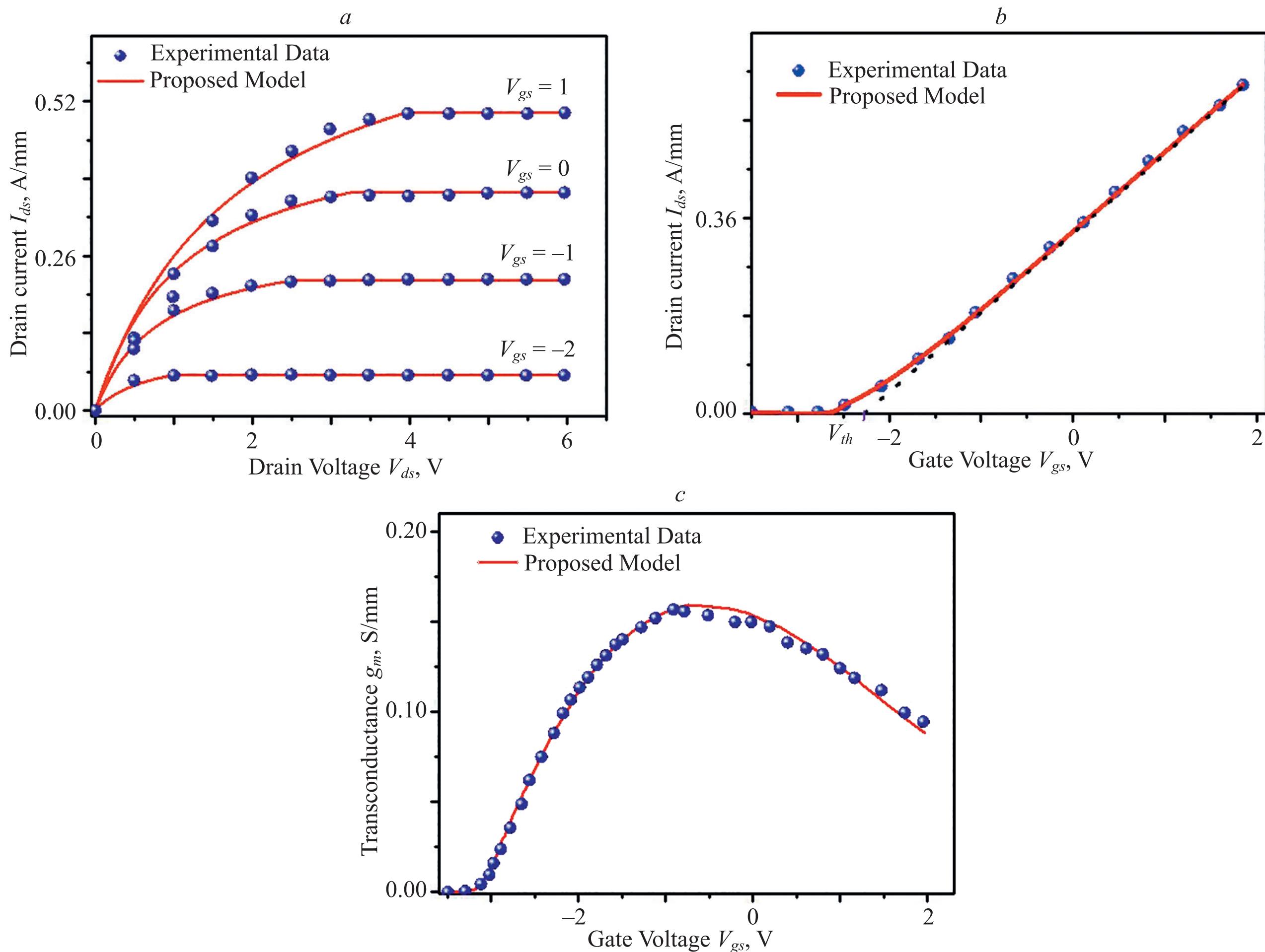

Fig. 3. Variation of the drain current I_{ds} as a function of: the drain voltage V_{ds} for different gate voltage values V_{gs} (*a*) and gate voltage V_{gs} by fixing the drain voltage V_{ds} at 5V (*b*); variation of the transconductance g_m as a function of gate voltage V_{gs} (*c*)

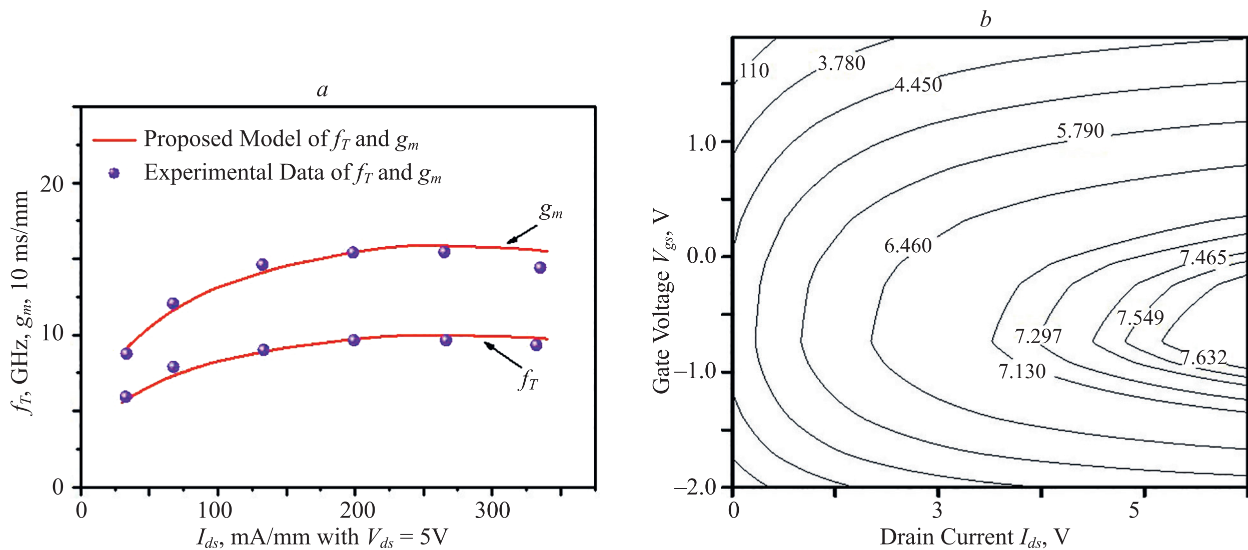

Fig. 4. Cut-off frequencies vs. drain current I_{ds} at drain voltage V_{ds} at 5V (Z = 2×75 μm) (*a*); dependence of the cut-off frequency f_T with polarization voltages V_{gs} and V_{ds} (*b*)

of 250 mA/mm, where the maximum of transcanductance is located.

Fig. 4, *b* presents the dependence of the cut-off frequency f_T on the gate and drain polarization voltages. It is obvious that the cut-off frequency rises with the gate voltage and decreases after reaching a maximum. Also, this cut-off frequency increases with the applied drain voltage. This is due to the impact of the gate voltage on the depth of the potential well and favors important diffusion of free electrons from the semiconductor donors.

Conclusion

In summary, we have studied a new analytical model of the drain current and small signal parameters of AlGaN-GaN HEMTs devices and considered the nonlinear polarization effect using the 2-DEG channel current equation. With the help of the charge control model, a detailed investigation of different functioning regimes of the HEMT transistor has been conducted. In this work, we optimized the difference between the proposed model and the experimental data. This later extracted from the current-voltage characteristics evidence that this model is useful for the prediction of drain current. Basing on this model, we can calculate the values of the transconductance g_m and the cut-off frequency f_T. These results showed that the simulation model is satisfactory and consistent with the experimental measurements, evidencing the validity of our proposed model.

References

1. Liu J., Guo Y., Zhang J., Yao J., Huang X., Huang C., Huang Z., Yang K. Analytical model for the potential and electric field distributions of AlGaN/GaN HEMTs with gate connected FP based on Equivalent Potential Method. *Superlattices and Microstructures*, 2020, vol. 138, pp. 106327. https://doi.org/10.1016/j.spmi.2019.106327
2. Rashmi, Haldar S., Gupta R.S. 2-D analytical model for current-voltage characteristics and output conductance of AlGaN/GaN MODFET. *Microwave and Optical Technology Letters*, 2001, vol. 29, no. 2, pp. 117–123. https://doi.org/10.1002/mop.1102
3. Mohanbabu A., Anbuselvan N., Mohankumar N., Godwinraj D., Sarkar C.K. Modeling of sheet carrier density and microwave frequency characteristics in Spacer based AlGaN/AlN/GaN HEMT devices. *Solid-State Electronics*, 2014, vol. 91, pp. 44–52. https://doi.org/10.1016/j.sse.2013.09.009
4. Jebalin B.K., Rekh A.S., Prajoon P., Godwinraj D., Kumar N.M., Nirmal D. Unique model of polarization engineered AlGaN/GaN based HEMTs for high power applications. *Superlattices and Microstructures*, 2015, vol. 78, pp. 210–223. https://doi.org/10.1016/j.spmi.2014.10.038
5. Rashmi, Kranti A., Haldar S., Gupta R.S. An accurate charge control model for spontaneous and piezoelectric polarization dependent two-dimensional electron gas sheet charge density of lattice-mismatched AlGaN/GaN HEMTs. *Solid-State Electronics*, 2002, vol. 46, no. 5, pp. 621–630. https://doi.org/10.1016/S0038-1101(01)00332-X
6. Kumar S.P., Agrawal A., Kabra S., Gupta M., Gupta R.S. An analysis for AlGaN/GaN modulation doped field effect transistor using

Литература

1. Liu J., Guo Y., Zhang J., Yao J., Huang X., Huang C., Huang Z., Yang K. Analytical model for the potential and electric field distributions of AlGaN/GaN HEMTs with gate connected FP based on Equivalent Potential Method // Superlattices and Microstructures. 2020. V. 138. P. 106327. https://doi.org/10.1016/j.spmi.2019.106327
2. Rashmi, Haldar S., Gupta R.S. 2-D analytical model for current-voltage characteristics and output conductance of AlGaN/GaN MODFET // Microwave and Optical Technology Letters. 2001. V. 29. N 2. P. 117–123. https://doi.org/10.1002/mop.1102
3. Mohanbabu A., Anbuselvan N., Mohankumar N., Godwinraj D., Sarkar C.K. Modeling of sheet carrier density and microwave frequency characteristics in Spacer based AlGaN/AlN/GaN HEMT devices // Solid-State Electronics. 2014. V. 91. P. 44–52. https://doi.org/10.1016/j.sse.2013.09.009
4. Jebalin B.K., Rekh A.S., Prajoon P., Godwinraj D., Kumar N.M., Nirmal D. Unique model of polarization engineered AlGaN/GaN based HEMTs for high power applications. Superlattices and Microstructures. 2015. V. 78. P. 210–223. https://doi.org/10.1016/j.spmi.2014.10.038
5. Rashmi, Kranti A., Haldar S., Gupta R.S. An accurate charge control model for spontaneous and piezoelectric polarization dependent two-dimensional electron gas sheet charge density of lattice-mismatched AlGaN/GaN HEMTs // Solid-State Electronics. 2002. V. 46. N 5. P. 621–630. https://doi.org/10.1016/S0038-1101(01)00332-X
6. Kumar S.P., Agrawal A., Kabra S., Gupta M., Gupta R.S. An analysis for AlGaN/GaN modulation doped field effect transistor using

accurate velocity-field dependence for high power microwave frequency applications. *Microelectronics Journal*, 2006, vol. 37, no. 11, pp. 1339–1346. https://doi.org/10.1016/j.mejo.2006.07.003

7. Ambacher O., Smart J., Shealy J.R., Weimann N.G., Chu K., Murphy M., Schaff W.J., Eastman L.F., Dimitrov R., Wittmer L., Stutzman M., Reiger W., Hilsenbeck J. Two-dimensional electron gases induced by spontaneous and piezoelectric polarization charges in N- and Ga-face AlGaN/GaN heterostructures. *Journal of Applied Physics*, 1999, vol. 85, no. 6, pp. 3222–3233. https://doi.org/10.1063/1.369664
8. Fiorentini V., Bernardini F., Ambacher O. Evidence for nonlinear macroscopic polarization in III-V nitride alloy heterostructures. *Applied Physics Letters*, 2002, vol. 80, no. 7, pp. 1204–1206. https://doi.org/10.1063/1.369664 ttps://doi.org/10.1063/1.1448668
9. Chattopadhyay M.K., Tokekar S. Temperature and polarization dependent polynomial based non-linear analytical model for gate capacitance of AlmGa1-mN/GaN MODFET. *Solid-State Electronics*, 2006, vol. 50, no. 2, pp. 220–227. https://doi.org/10.1016/j.sse.2005.10.016
10. Tyagi R.K., Ahlawat A., Pandey M., Pandey S. An analytical two-dimensional model for AlGaN/GaN HEMT with polarization effects for high power applications. *Microelectronics Journal*, 2007, vol. 38, no. 8-9, pp. 877–883. https://doi.org/10.1016/j.mejo.2007.07.003
11. Li M., Wang Y. 2-D Analytical model for current–voltage characteristics and transconductance of AlGaN/GaN MODFETs. *IEEE Transactions on Electron Devices*, 2008, vol. 55, no. 1, pp. 261–267. https://doi.org/10.1109/TED.2007.911076
12. Huque M.A., Eliza S.A., Rahman T., Huq H.F., Islam S.K. Temperature dependent analytical model for current–voltage characteristics of AlGaN/GaN power HEMT. *Solid-State Electronics*, 2009, vol. 53, no. 3, pp. 341–348. https://doi.org/10.1016/j.sse.2009.01.004
13. Rathi S., Jogi J., Gupta M., Gupta R.S. Modeling of hetero-interface potential and threshold voltage for tied and separate nanoscale InAlAs–InGaAs symmetric double-gate HEMT. *Microelectronics Reliability*, 2009, vol. 49, no. 12, pp. 1508–1514. https://doi.org/10.1016/j.microrel.2009.07.044
14. Mukhopadhyay P., Banerjee U., Bag A., Ghosh S., Biswas D. Influence of growth morphology on electrical and thermal modeling of AlGaN/GaN HEMT on sapphire and silicon. *Solid-State Electronics*, 2015, vol. 104, pp. 101–108. https://doi.org/10.1016/j.sse.2014.11.017
15. Gangwani P., Kaur R., Pandey S., Haldar S., Gupta M., Gupta R.S. Modeling and analysis of fully strained and partially relaxed lattice mismatched AlGaN/GaN HEMT for high temperature applications. *Superlattices and Microstructures*, 2008, vol. 44, no. 6, pp. 781–793. https://doi.org/10.1016/j.spmi.2008.07.004
16. Chattopadhyay M.K., Tokekar S. Thermal model for dc characteristics of AlGaN/GaN hemts including self-heating effect and non-linear polarization. *Microelectronics Journal*, 2008, vol. 39, no. 10, pp. 1181–1188. https://doi.org/10.1016/j.mejo.2008.01.043
17. Madhulika, Malik A., Jain N., Mishra M., Kumar S., Rawal D.S., Singh A.K. Nanoscale structural parameters based analytical model for GaN HEMTs. *Superlattices and Microstructures*, 2019, vol. 130, pp. 267–276. https://doi.org/10.1016/j.spmi.2019.04.040
18. Wu Y.F., Keller S., Kozodoy P., Keller B.P., Parikh P., Kapolnek D., Denbaars S.P., Mishra U.K. Bias dependent microwave performance of AlGaN/GaN MODFET's up to 100 V. *IEEE Electron Device Letters*, 1997, vol. 18, no. 6, pp. 290–292. https://doi.org/10.1109/55.585362
19. Dasgupta N., Dasgupta A. An analytical expression for sheet carrier concentration vs gate voltage for HEMT modelling. *Solid-State Electronics*, 1993, vol. 36, no. 2, pp. 201–203. https://doi.org/10.1016/0038-1101(93)90140-L

•

accurate velocity-field dependence for high power microwave frequency applications // Microelectronics Journal. 2006. V. 37. N 11. P. 1339–1346. https://doi.org/10.1016/j.mejo.2006.07.003

7. Ambacher O., Smart J., Shealy J.R., Weimann N.G., Chu K., Murphy M., Schaff W.J., Eastman L.F., Dimitrov R., Wittmer L., Stutzman M., Reiger W., Hilsenbeck J. Two-dimensional electron gases induced by spontaneous and piezoelectric polarization charges in N- and Ga-face AlGaN/GaN heterostructures // Journal of Applied Physics. 1999. V. 85. N 6. P. 3222–3233. https://doi.org/10.1063/1.369664
8. Fiorentini V., Bernardini F., Ambacher O. Evidence for nonlinear macroscopic polarization in III-V nitride alloy heterostructures // Applied Physics Letters. 2002. V. 80. N 7. P. 1204–1206. https://doi.org/10.1063/1.1448668
9. Chattopadhyay M.K., Tokekar S. Temperature and polarization dependent polynomial based non-linear analytical model for gate capacitance of AlmGa1-mN/GaN MODFET // Solid-State Electronics. 2006. V. 50. N 2. P. 220–227. https://doi.org/10.1016/j.sse.2005.10.016
10. Tyagi R.K., Ahlawat A., Pandey M., Pandey S. An analytical two-dimensional model for AlGaN/GaN HEMT with polarization effects for high power applications // Microelectronics Journal. 2007. V. 38. N 8-9. P. 877–883. https://doi.org/10.1016/j.mejo.2007.07.003
11. Li M., Wang Y. 2-D Analytical model for current–voltage characteristics and transconductance of AlGaN/GaN MODFETs // IEEE Transactions on Electron Devices. 2008. V. 55. N 1. P. 261–267. https://doi.org/10.1109/TED.2007.911076
12. Huque M.A., Eliza S.A., Rahman T., Huq H.F., Islam S.K. Temperature dependent analytical model for current–voltage characteristics of AlGaN/GaN power HEMT // Solid-State Electronics. 2009. V. 53. N 3. P. 341–348. https://doi.org/10.1016/j.sse.2009.01.004
13. Rathi S., Jogi J., Gupta M., Gupta R.S. Modeling of hetero-interface potential and threshold voltage for tied and separate nanoscale InAlAs–InGaAs symmetric double-gate HEMT // Microelectronics Reliability. 2009. V. 49. N 12. P. 1508–1514. https://doi.org/10.1016/j.microrel.2009.07.044
14. Mukhopadhyay P., Banerjee U., Bag A., Ghosh S., Biswas D. Influence of growth morphology on electrical and thermal modeling of AlGaN/GaN HEMT on sapphire and silicon // Solid-State Electronics. 2015. V. 104. P. 101–108. https://doi.org/10.1016/j.sse.2014.11.017
15. Gangwani P., Kaur R., Pandey S., Haldar S., Gupta M., Gupta R.S. Modeling and analysis of fully strained and partially relaxed lattice mismatched AlGaN/GaN HEMT for high temperature applications // Superlattices and Microstructures. 2008. V. 44. N 6. P. 781–793. https://doi.org/10.1016/j.spmi.2008.07.004
16. Chattopadhyay M.K., Tokekar S. Thermal model for dc characteristics of AlGaN/GaN hemts including self-heating effect and non-linear polarization // Microelectronics Journal. 2008. V. 39. N 10. P. 1181–1188. https://doi.org/10.1016/j.mejo.2008.01.043
17. Madhulika, Malik A., Jain N., Mishra M., Kumar S., Rawal D.S., Singh A.K. Nanoscale structural parameters based analytical model for GaN HEMTs // Superlattices and Microstructures. 2019. V. 130. P. 267–276. https://doi.org/10.1016/j.spmi.2019.04.040
18. Wu Y.F., Keller S., Kozodoy P., Keller B.P., Parikh P., Kapolnek D., Denbaars S.P., Mishra U.K. Bias dependent microwave performance of AlGaN/GaN MODFET's up to 100 V // IEEE Electron Device Letters. 1997. V. 18. N 6. P. 290–292. https://doi.org/10.1109/55.585362
19. Dasgupta N., Dasgupta A. An analytical expression for sheet carrier concentration vs gate voltage for HEMT modelling // Solid-State Electronics. 1993. V. 36. N 2. P. 201–203. https://doi.org/10.1016/0038-1101(93)90140-L

Authors

Azzeddine Farti — PhD, Associate Professor, Hassan II University of Casablanca, Casablanca, 20190, Morocco, https://orcid.org/0000-0002-8694-1471, azzeddine.farti-etu@etu.univh2c.ma

Abdelkader Touhami — D.Sc, Full Professor, Hassan II University of Casablanca, Casablanca, 20190, Morocco, SC 8158211000, https://orcid.org/0000-0001-8582-1884, abdelkadertouhami2016@gmail.com

Авторы

Фарти Азеддин — PhD, доцент, Университет Хасана II, Факультет наук Касабланки, Касабланка, 20190, Марокко, https://orcid.org/0000-0002-8694-1471, azzeddine.farti-etu@etu.univh2c.ma

Тухами Абделькадер — D.Sc, профессор, профессор, Университет Хасана II, Факультет наук Касабланки, Касабланка, 20190, Марокко, SC 8158211000, https://orcid.org/0000-0001-8582-1884, abdelkadertouhami2016@gmail.com

Received 08.09.2021
Approved after reviewing 03.12.2021
Accepted 28.01.2022

Статья поступила в редакцию 08.09.2021
Одобрена после рецензирования 03.12.2021
Принята к печати 28.01.2022